transport occurs across a constant concentration gradient of oxidized redox sites. Thus the conducting polymer behaves like a redox polymer in this case.[12]

Rotating disk voltammetry is an excellent method for investigating the potential-dependent conductivity of moderately conducting polymers. From the perspective of using these materials as mediators in electroanalysis or electrosynthesis, this method has the advantage that conductivity measurements can be made under conditions similar to those of the application. The new treatment presented here is more accurate at potentials close to, and above, the formal potential than our previously reported method.[2,10]

The conductivity results presented in Figure 4 are of value in the interpretation of impedance measurements on poly-MPMP$^+$. The ionic and electronic conductivities of oxidized poly-MPMP$^+$ are very similar, and it has therefore been difficult to assign values from impedance measurements.[11] The new in situ electronic conductivities reported here indicate that fully oxidized poly-MPMP$^+$ is approximately an order of magnitude more conductive than previously reported.[2]

Acknowledgment. Financial support from the Natural Sciences and Engineering Research Council of Canada (NSERC) and Memorial University is gratefully acknowledged.

Registry No. MPMPBF$_4$, 122202-27-1; poly-MPMP$^+$, 125357-35-9; CH$_3$CN, 75-05-8; Et$_4$NBF$_4$, 429-06-1; Pt, 7440-06-4; ferrocene, 102-54-5.

---

[12] Pickup, P. G.; Murray, R. W. *J. Am. Chem. Soc.* **1983**, *105*, 4510–4514.

Crystal Chemistry of Colquiriite-Type Fluorides

Yaobo Yin and Douglas A. Keszler*

Department of Chemistry and Center for Advanced Materials Research, Gilbert Hall 153,
Oregon State University, Corvallis, Oregon 97331-4003

Received December 4, 1991. Revised Manuscript Received January 27, 1992

Crystal structures of six fluorides in the family LiMM′F$_6$ (M = Sr or Ca; M′ = Al, Ga, or Cr) have been refined with single-crystal X-ray diffraction data. Each compound crystallizes in trigonal space group $P\bar{3}1c$ (Z = 2) as an ordered derivative of the Li$_2$ZrF$_6$ structure type. Cell parameters: LiCaAlF$_6$, a = 5.007 (1), c = 9.641 (1) Å; LiCaGaF$_6$, a = 5.079 (3), c = 9.752 (2) Å; LiCaCrF$_6$, a = 5.098 (2), c = 9.775 (1) Å; LiSrAl$_{0.59(1)}$Cr$_{0.41(1)}$F$_6$, a = 5.117 (3), c = 10.275 (1), Å; LiSrGaF$_6$, a = 5.154 (1), c = 10.321 (2) Å; LiSrCrF$_6$, a = 5.174 (5), c = 10.369 (1) Å. Each cation occupies a deformed octahedral site in a distorted hexagonally closest-packed F$^-$ arrangement; the distortions of the D$_3$ M′ site are examined in detail.

Introduction

Because of their long operational lifetimes, reliable and efficient flash lamp or diode pumping, and high beam quality at high average power levels, tunable solid-state lasers can offer considerable advantages over conventional dye lasers. Recently, two new tunable laser materials, Cr^{3+}:LiCaAlF$_6$ and Cr^{3+}:LiSrAlF$_6$, were reported.[1,2] These materials exhibit high intrinsic lasing efficiency, low thermal lensing, and excellent resistance to UV solarization. Each host, however, exhibits unique lasing and optical characteristics. For example, the Ca derivative exhibits a higher intrinsic efficiency of 67% vs 53% for the Sr derivative, a smaller π emission cross section of 1.3 × 10^{-20} cm^2 vs 4.8 × 10^{-20} cm^2, and a longer emission lifetime of 170 μs vs 67 μs. These characteristics are determined by the static and dynamic characteristics of the hosts and, in particular, the characteristics of the Al dopant site. In a recent account we described the static distortions of the AlF$_6$ site in the host LiSrAlF$_6$ that contribute to the heightened cross section and shorter lifetime of the Cr^{3+} optical emission.[3]

In this report we present crystal data on colquiriite (LiCaAlF$_6$)[4] and its derivatives LiCaCrF$_6$, LiCaGaF$_6$, LiSrAl$_{0.59(1)}$Cr$_{0.41(1)}$F$_6$, LiSrCrF$_6$, and LiSrGaF$_6$, some of which are being developed as new laser materials.

Experimental Section

The single crystals of LiCaCrF$_6$, LiSrGaF$_6$, LiCaAlF$_6$, and LiSrAl$_{0.59}$Cr$_{0.41}$F$_6$ were grown at Lawrence Livermore National Laboratory, and the single crystals of LiCaGaF$_6$ and LiSrCrF$_6$ were prepared at Oregon State University. Reagents used for crystal growth at OSU were the following: LiF (AESAR, 99.99%), CaO (AESAR, 99.95%), Ga$_2$O$_3$ (AESAR, 99.999%), SrF$_2$ (Cerac, 99%), and Cr$_2$O$_3$ (Johnson Matthey, 99%). A powder of LiCaGaF$_6$ was prepared by passing HF(g) (Matheson, 99.9%) over a stoichiometric mixture of the starting reagents at 700 °C for 1 h followed by annealing at the same temperature for 12 h. The single crystal was grown by maintaining the melt at 850 °C for 20 min and then rapidly cooling to and annealing at 700 °C for 24 h. A colorless single crystal of dimensions 0.1 × 0.1 × 0.1 mm was physically separated from the solidified melt. The single crystal of LiSrCrF$_6$ having dimensions 0.1 × 0.08 × 0.1 mm was obtained by passing HF(g) over the mixture SrF$_2$:1.5LiF:0.75Cr$_2$O$_3$ at 650 °C for 2 h and then heating to 810 °C and cooling to 700 °C at a rate of 12 °C/h.

The single crystals were mounted on glass fibers and analyzed on a Rigaku AFC6R diffractometer. Cell parameters were obtained from least-squares refinement of the setting angles of 10–19

---

* To whom correspondence should be addressed.

[1] Payne, S. A.; Chase, L. L.; Newkirk, H. W.; Smith, L. K.; Krupke, W. F. *IEEE J. Quantum Electron.* **1988**, *24*, 2243.

[2] Payne, S. A.; Chase, L. L.; Smith, L. K.; Kway, W. L.; Newkirk, H. W. *J. Appl. Phys.* **1989**, *66*, 1051.

[3] Schaffers, K. I.; Keszler, D. A. *Acta Crystallogr., Sect. C* **1991**, *47*, 18.

[4] Viebahn, V. W. *Z. Anorg. Allg. Chem.* **1971**, *386*, 335.

0897-4756/92/2804-0645$03.00/0 © 1992 American Chemical Society

Table I. Crystal Data and Experimental Conditions for Colquiriite-Type Fluorides[a]

	$LiCaAlF_6$	$LiCaGaF_6$	$LiCaCrF_6$	$LiSrAl_{0.6}Cr_{0.4}F_6$	$LiSrGaF_6$	$LiSrCrF_6$
FW, amu	187.99	230.73	213.01	245.54	278.27	260.55
space group	$P\bar{3}1c$	$P\bar{3}1c$	$P\bar{3}1c$	$P\bar{3}1c$	$P\bar{3}1c$	$P\bar{3}1c$
a, Å	5.007 (1)	5.079 (1)	5.098 (1)	5.117 (2)	5.154 (1)	5.174 (1)
c, Å	9.641 (2)	9.752 (2)	9.775 (4)	10.275 (2)	10.320 (1)	10.369 (1)
c/a	1.926	1.920	1.917	2.008	2.002	2.004
V, Å^3	209.3 (1)	217.9 (1)	220.0 (1)	233.0 (1)	237.43 (8)	240.34 (6)
Z			2			
ρ_{calc}, g/cm^{-3}	2.983	3.517	3.215		3.892	3.600
μ, cm^{-1}	17.13	74.84	37.19	124.33	165.92	130.11
data collected	$h,\pm k,\pm l$	$h,\pm k,\pm l$	$h,\pm k,\pm l$	$h,\pm k,\pm l$	$h,\pm k,\pm l$	$h,\pm k,\pm l$
$\sin \theta_{max}/\lambda$	0.7035	0.7035	0.8759	0.7035	0.8566	0.7035
transmission factors	0.86–1.20	0.96–1.08	0.85–1.12	0.83–1.21	0.84–1.34	0.65–1.00
R_{int}	0.051	0.046	0.050	0.055	0.086	0.064
$R_w(F_o)$	0.024	0.025	0.056	0.034	0.034	0.024
$R(F_o)$ for $F_o^2 > 3\sigma(F_o^2)$	0.021	0.025	0.041	0.033	0.026	0.018

[a] All data collection at 296 K with graphite monochromated Mo Kα ($\lambda(K\alpha) = 0.71069$ Å) radiation.

Table II. Atomic Parameters of Colquiriite-Type Fluorides $LiMM'F_6$[a]

		M = Ca, M′ = Al	M = Ca, M′ = Ga	M = Ca, M′ = Cr	M = Sr, M′ = Ga	M = Sr, M′ = Cr	M = Sr, M′ = Al,Cr
Li	B_{eq}	1.2 (1)	1.5 (2)	1.6 (3)	1.3 (2)	1.0 (2)	1.3 (4)
M	B_{eq}	0.69 (2)	0.65 (2)	0.89 (2)	0.99 (1)	0.88 (2)	0.78 (2)
M′	B_{eq}	0.50 (2)	0.51 (1)	0.75 (2)	0.81 (1)	0.70 (2)	0.56 (4)
F	x	0.0306 (1)	0.0201 (3)	0.0185 (3)	0.0211 (4)	0.0202 (3)	0.0277 (4)
	y	0.3768 (1)	0.3688 (2)	0.3653 (3)	0.3795 (4)	0.3653 (3)	0.3835 (5)
	z	−0.1434 (2)	−0.1407 (1)	−0.1403 (1)	−0.1459 (1)	−0.1458 (1)	−0.1469 (2)
	B_{eq}	0.99 (2)	1.01 (4)	1.24 (4)	1.51 (5)	1.43 (5)	1.40 (7)

[a] Li is located in Wyckoff position 2*c* ($^1/_3,^2/_3,^1/_4$), M′ in **2b** ($^2/_3,^1/_3,^1/_4$), and M in 2*a* (0,0,0).

Table III. Interatomic Distances for Colquiriite Derivatives

compound	dist, Å			
$LiCaAlF_6$	Ca–F	2.281 (4)	Li–F	2.006 (7)
	Al–F	1.805 (6)		
$LiCaGaF_6$	Ca–F	2.283 (1)	Li–F	2.017 (1)
	Ga–F	1.884 (1)		
$LiCaCrF_6$	Ca–F	2.277 (1)	Li–F	2.025 (2)
	Cr–F	1.903 (1)		
$LiSrAlF_6$[a]	Sr–F	2.424 (1)	Li–F	2.018 (6)
	Al–F	1.795 (5)		
$LiSrGaF_6$	Sr–F	2.428 (2)	Li–F	2.028 (2)
	Ga–F	1.885 (1)		
$LiSrCrF_6$	Sr–F	2.425 (2)	Li–F	2.039 (1)
	Cr–F	1.902 (1)		
$LiSrAl_{0.59}Cr_{0.41}F_6$	Sr–F	2.423 (3)	Li–F	2.032 (2)
	Al(Cr)–F	1.845 (2)		

[a] Reference 3.

centered reflections in the range $30 \leq 2\theta \leq 36°$. On the basis of the systematic absence *hhl*, $l = 2n + 1$, and successful refinement, each crystal was found to crystallize in space group $P\bar{3}1c$ (No. 163).

All calculations were performed on a microVAX II computer with programs from the TEXSAN crystallographic software package.[5] The atoms Li, M (M = Sr or Ca), and M′ (M′ = Al, Ga, or Cr) were placed by comparison to the isostructural compounds $LiCaAlF_6$ and $LiSrAlF_6$. The position of the F atom in each derivative was determined by examining difference electron density maps. Following refinement of each structure with isotropic thermal parameters, the data were corrected for absorption with the program DIFABS.[6] Final least-squares refinement included anisotropic thermal parameters on each atom. In the mixed crystal $LiSr(Al,Cr)F_6$ the occupancy of the M′ site was refined as two atoms disordered on one site with the total occupancy constrained to 1. Final difference electron density maps were featureless with maximum peaks corresponding to <0.5% of a Ca or Sr atom.

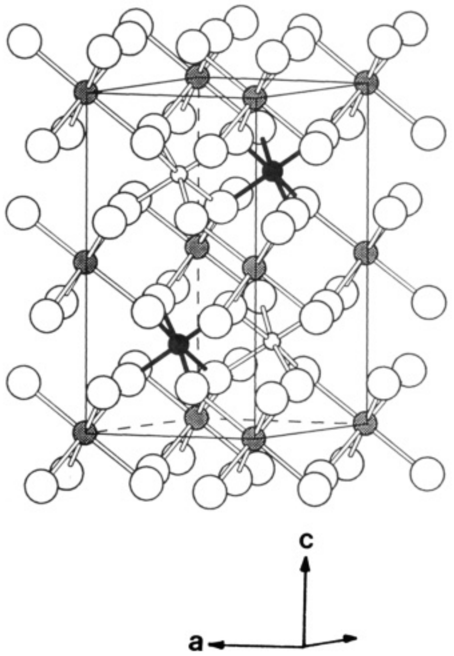

Figure 1. Drawing of the colquiriite structure. Large open circles represent F atoms. Small filled circles represent Al atoms, small open circles Li atoms, and small shaded circles Sr atoms, here, and in Figure 2.

Crystal data and final atomic parameters are listed in Tables I and II, respectively, and anisotropic thermal parameters and structure factors are arranged in Tables S-1 and S-2, respectively, in the supplementary material (see paragraph at end of paper).

Discussion

Each of the materials is isostructural to the mineral colquiriite, $LiCaAlF_6$, which is a derivative of the Li_2ZrF_6 structure type. In this trigonal structure, Figure 1, the cations occupy distorted octahedral environments between planes of approximately closest-packed fluoride anions that extend in the *ab* plane. Considering the general formula

---

[5] Molecular Structure Corporation. TEXSAN. TEXRAY Structure Analysis Package. MSC, 3200A Research Forest Drive, The Woodlands, TX 77381.

[6] Walker, N.; Stuart, D. *Acta Crystallogr., Sect. A* **1983**, *39*, 158.

Table IV. Interatomic Angles for Colquiriite Derivatives

compound	angles, deg			
$LiCaAlF_6$	F–Al–F	90.81 (3)	F–Al–F	91.76 (4)
	F–Al–F	86.72 (4)		
	F–Ca–F	92.93 (3)		
	F–Li–F	96.13 (3)	F–Li–F	92.34 (4)
	F–Li–F	76.31 (3)		
	Ca–F–Al	133.78 (3)	Ca–F–Li	122.60 (3)
	Al–F–Li	98.48 (3)		
$LiCaGaF_6$	F–Ga–F	91.14 (6)	F–Ga–F	91.87 (7)
	F–Ga–F	85.99 (8)		
	F–Ca–F	92.41 (5)		
	F–Li–F	94.65 (5)	F–Li–F	92.19 (7)
	F–Li–F	79.14 (7)		
	Ca–F–Ga	132.25 (6)	Ca–F–Li	124.87 (6)
	Ga–F–Li	97.43 (5)		
$LiCaCrF_6$	F–Cr–F	91.34 (5)	F–Cr–F	91.29 (7)
	F–Cr–F	86.14 (7)		
	F–Ca–F	92.53 (5)		
	F–Li–F	94.54 (5)	F–Li–F	91.60 (8)
	F–Li–F	79.83 (6)		
	Ca–F–Cr	132.30 (9)	Ca–F–Li	125.48 (5)
	Cr–F–Li	97.01 (6)		
$LiSrAlF_6$[a]	F–Al–F	90.32 (7)	F–Al–F	94.18 (7)
	F–Al–F	85.48 (6)		
	F–Sr–F	95.00 (1)		
	F–Li–F	96.25 (4)	F–Li–F	94.69 (5)
	F–Li–F	74.27 (1)		
	Sr–F–Al	133.22 (2)	Sr–F–Li	121.47 (8)
	Al–F–Li	100.12 (2)		
$LiSrGaF_6$	F–Ga–F	90.72 (1)	F–Ga–F	94.3 (2)
	F–Ga–F	84.6 (2)		
	F–Sr–F	94.42 (6)		
	F–Li–F	94.6 (1)	F–Li–F	94.5 (1)
	F–Li–F	77.47 (1)		
	Sr–F–Ga	131.5 (2)	Sr–F–Li	124.0 (1)
	Ga–F–Li	98.95 (8)		
$LiSrCrF_6$	F–Cr–F	90.89 (6)	F–Cr–F	93.6 (1)
	F–Cr–F	84.93 (8)		
	F–Sr–F	94.76 (6)		
	F–Li–F	94.50 (5)	F–Li–F	93.9 (1)
	F–Li–F	78.06 (7)		
	Sr–F–Cr	131.80 (7)	Sr–F–Li	124.54 (6)
	Cr–F–Li	98.50 (6)		
$LiSr(Al,Cr)F_6$	F–Al,Cr–F	90.3 (1)	F–(Al,Cr)–F	94.2 (1)
	F–(Al,Cr)–F	85.5 (1)		
	F–Sr–F	94.71 (8)		
	F–Li–F	95.29 (8)	F–Li–F	94.6 (1)
	F–Li–F	76.1 (1)		
	Sr–F–(Al,Cr)	132.6 (1)	Sr–F–Li	122.79 (9)
	(Al,Cr)–F–Li	99.2 (1)		

[a] Reference 3.

$LiMM'F_6$ where M = Ca or Sr and M′ = Al, Ga, or Cr, the atoms stack in the sequence ···F(Li,M′)FMF···, i.e., the Li and M′ atoms are sandwiched together between the same anionic layers, and the M atoms stand alone in adjacent layers. The Li- and M′-centered octahedra share edges with one another and vertexes with the Sr-centered octahedra.

Interatomic distances and angles for the structures are listed in Tables III and IV, respectively. M′–F distances increase in the order Al–F < Ga–F < Cr–F for both the Ca and Sr derivatives. Ca–F and Sr–F distances are constant with changes in the M′ atom, while a trend of larger Li–F distances with longer M′–F distances is evident in both the Ca and Sr series; this trend is consistent with the height of the (Li,M′)-centered sandwich which expands as the size of the M′ atom increases.

The D_3 sites of the atoms M′ exhibit small, but important, distortions from O_h symmetry. In Table IV, the first F–M′–F angle corresponds to two F atoms in the same trigonal plane, while the second and third correspond to interactions in opposite planes. The deviations from orthogonality for the latter two interactions are associated with the relative orientations of the trigonal F planes perpendicular to the C_3 *c* axis. These planes are twisted to afford angles, θ, 1, that deviate from the ideal 60°, Table V. The greatest change in the magnitude of the angle occurs between the Ca and Sr derivatives, where larger angles are associated with the larger Sr atom. In the series Al, Ga, and Cr, the Ga derivatives exhibit the larger distortions, while the sites in the Al and Cr derivatives are comparable. As noted in the report on the compound $LiSrAlF_6$,[3] the distortion results from displacements of the F atoms from an ideal closest packing (Figure 2). Trigonal hollows of F atoms expand in the presence of the large Ca or Sr atoms. Since each F atom interacts with one Li atom, one M atom, and one M′ atom, this expansion is coupled with an electrostatic relaxation toward the more highly charged M'^{3+} cations. Because the M atoms about an $M'F_6$ site define a trigonal prism, the two trigonal F planes rotate in opposite directions. The primary effect of this distortion is the introduction of an odd-parity component to the crystal field at the Cr^{3+} dopant site. The sensitivity of the optical properties to this distortion is noted by the $(\Delta\theta)^2$ $[\Delta\theta = \theta - 60°]$ dependence of the radiative rates.[7]

Table V. Twist Angles of Colquiriite-Type Fluorides

compound	$\Delta\theta$[a]	compound	$\Delta\theta$[a]
$LiCaAlF_6$	4.3	$LiSrGaF_6$	8.2
$LiCaGaF_6$	5.0	$LiSrCrF_6$	7.4
$LiCaCrF_6$	4.3	$LiSrAl_{0.59}Cr_{0.41}F_6$	7.5
$LiSrAlF_6$[b]	7.2		

[a] $\Delta\theta = \theta - 60°$. [b] Reference 3.

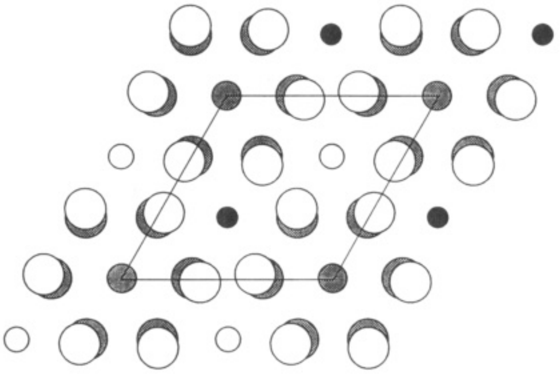

Figure 2. Comparison of F closest packing with F packing in the structure of $LiSrGaF_6$ by projection onto (001). Ideal F closest packing is represented by large shaded circles.

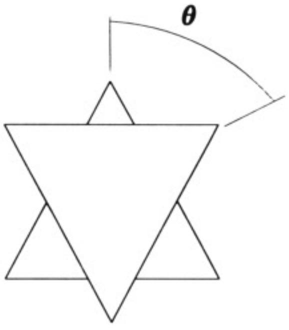

1

The stoichiometry of the mixed crystal $LiSrAl_{0.59}Cr_{0.41}F_6$ compares well to that of the melt, $LiSrAl_{0.6}Cr_{0.4}F_6$. The results are consistent with congruency of the sample and

---

[7] Payne, S. A.; Chase, L. L.; Wilke, G. D. *J. Lumin.* **1989**, *44*, 167.

a segregation coefficient = 1. Also, significant doping levels of Cr^{3+} ions can be achieved in the Al system while maintaining high crystal quality. In this regard, the solution series $LiSr_{1-x}Ba_xAlF_6$ should be examined for crystal quality as a function of the level of Ba substitution and to determine the maximum value of x consistent with formation of the colquiriite structure type since $LiBaAlF_6$ crystallizes in a different structure.[8] The presence of Ba atoms should afford larger twist angles and higher cross sections for Cr^{3+} optical emission.

Acknowledgment. We thank Dr. Stephen A. Payne of Lawrence Livermore Laboratory for supplying crystals. This work was supported by the US National Science Foundation, DMR-8814432. D.A.K. is grateful to the Alfred P. Sloan Foundation for a fellowship, 1989–1991.

Registry No. $LiCaAlF_6$, 35362-46-0; $LiCaGaF_6$, 35361-72-9; $LiCaCrF_6$, 29467-85-4; $LiSrAl_{0.59}Cr_{0.41}F_6$, 141017-13-2; $LiSrGaF_6$, 35361-73-0; $LiSrCrF_6$, 29661-32-3.

Supplementary Material Available: Listing of anisotropic thermal parameters (Table S-1, 2 pages); listing of calculated and observed structure factors (Table S-2, 14 pages). Ordering information is given on any current masthead page.

---

(8) Babel, D. *Z. Anorg. Allg. Chem.* **1974**, *406*, 23.

Thermodynamic Analysis of the Thermal Nitridation of Aluminum Oxide by Ammonia and Methane

Beng Jit Tan,[†,‡] Youming Xiao,[†] and Steven L. Suib*[,†,‡,§]

Department of Chemistry, U-60, University of Connecticut, Storrs, Connecticut 06269-3060;
Institute of Materials Science, University of Connecticut, Storrs, Connecticut 06269; and
Department of Chemical Engineering, U-60, University of Connecticut,
Storrs, Connecticut 06269

Francis S. Galasso

United Technologies Research Center, East Hartford, Connecticut 06108

Received December 5, 1991. Revised Manuscript Received February 21, 1992

Thermodynamic calculations were performed using the SOLGASMIX-PV computer program to determine the possibility of converting aluminum oxide to aluminum nitride using alumina, ammonia, and methane. Conversion diagrams were constructed for the Al_2O_3–NH_3–CH_4 system over a range of reaction conditions such as temperature, total system pressure, and reagent concentrations. The influence of excess hydrogen, based on thermodynamic considerations alone, was also investigated. Formation of a pure AlN phase was predicted in the range 1800–2000 K and total system pressures of 0.1–1.0 atm. Low pressure and excess hydrogen increase the conversion efficiencies of aluminum and nitrogen, thus favoring the formation of pure AlN.

Introduction

In recent years, there has been increasing interest in non-oxide ceramics such as silicon nitride and silicon carbide which possess high-temperature strength and corrosion resistance. Among these, aluminum nitride is currently of great technological importance because of its unique physical properties such as high thermal conductivity (170–320 W/(m K)), close to that of metals[1–6] and over 10 times that of Al_2O_3, low coefficient of thermal expansion (4–5 μm/(m °C)) comparable to silicon and SiC,[1,7] high electrical resistivity (4×10^{11} Ω cm) and high mechanical strength comparable to alumina ceramics. It is a covalent material with a wurtzite-type crystal structure,[8] which is difficult to sinter. Its elastic,[9] mechanical,[10] and electrical[11] properties and its reactions with metals[12,13] have been described.[14] It has extreme hardness (about 3500 kgf mm^{-2}) and a high melting point (2400 °C). AlN has superior physical properties over those of alumina ceramics. It has a low dielectric constant and loss and good mechanical properties and is nontoxic.[15–17] AlN is a semiconductor with a wide bandgap (E_g = 6.2 eV) with a variety of potential applications including electronic devices for high-temperature operation, surface acoustic wave devices, and short-wavelength optoelectronics.

Aluminum nitride powders can be synthesized using a variety of reactions. One of the more common methods for commerical powders is carbothermal reduction and nitridation.[18–21] This involves intimate mixing of alumina

---

[†] Department of Chemistry.

[‡] Institute of Materials Science.

[§] Department of Chemical Engineering.

* To whom correspondence should be addressed.

(1) Slack, G. A. *J. Phys. Chem. Solids* **1973**, *34*, 321.
(2) Suryanarayana, D. *J. Electron Packag.* **1989**, *111*, 192.
(3) Komeya, K. *Ceram. Bull.* **1984**, *63*, 1158.
(4) Iwasi, N. *Int. J. Hybrid Microelectron.* **1984**, *7*, 49.
(5) Iwasi, N.; Anzai, K.; Shimozaki, K. *Solid State Technol.* **1986**, *Oct*, 135.
(6) Kurokawa, Y.; Utsumi, K.; Takamizawa, H. *J. Am. Ceram. Soc.* **1988**, *71*, 588.
(7) Li, Z.; Bradt, R. C. *J. Am. Ceram. Soc.* **1986**, *69*, 863.
(8) Amma, E. L.; Jeffrey, G. A. *J. Chem. Phys.* **1961**, *34*, 252.
(9) Gerlich, R. D.; Dole, S. L.; Slack, G. A. *J. Phys. Chem. Solids*, **1986**, *47*, 437.
(10) De With, G.; Hattu, N. *J. Mater. Sci.* **1983**, *18*, 503.
(11) Zulfequar, M.; Kumar, A. *J. Mater. Sci. Lett.* **1986**, *5*, 1230.
(12) Rhee, S. K. *J. Am. Ceram. Soc.* **1970**, *53*, 639.
(13) Trontelj, M.; Kolar, D. *J. Am. Ceram. Soc.* **1978**, *61*, 204.
(14) Billy, M. *J. Mexmain Sprechsaal* **1985**, *118*, 245.
(15) Kurokawa, Y.; Utsumi, K.; Takamizawa, H.; Kamata, T.; Noguchi, S. *IEEE Trans. Compon. Hybrids, Manuf. Technol.* **1985**, *CHMT-8*, 248.
(16) Kurokawa, Y.; Hamaguchi, H.; Shimada, Y.; Utsumi, K.; Takamizawa, H. *NEC Res. Dev.* **1987**, *85*, 15.
(17) Kuramoto, N.; Taniguchi, H.; Aso, I. *IEEE Trans. Compon. Hybrids Manuf. Technol.* **1986**, *CHMT-9*, 386.

0897-4756/92/2804-0648$03.00/0 © 1992 American Chemical Society